Int J Adv Manuf Technol (2018) 94:2905–2917
DOI 10.1007/s00170-017-1095-2

ORIGINAL ARTICLE

Measurement and identification of geometric errors of translational axis based on sensitivity analysis for ultra-precision machine tools

Weichao Peng[1] · **Hongjian Xia**[1] · **Sujuan Wang**[1] · **Xindu Chen**[1]

Received: 17 April 2017 / Accepted: 12 September 2017 / Published online: 20 September 2017

Abstract Identification of geometric errors of translational axis is a key step to improve the accuracy of machine tools. However, during the procedure of measurement, installation errors of instruments are inevitable and should influence the measurement results. In order to avoid this and improve the reliability and accuracy of measurement, a novel identification measurement method is proposed. The errors of positioning and straightness of translational axis are measured by a laser interferometer in four installation positions. Twelve measured results are obtained, and then are used to identify six geometric errors of translation axis, based on the homogeneous transformation matrix and the least square method. Furthermore, an optimization method based on sensitivity analysis of the identification matrix is presented to obtain the optimum installation positions of the laser interferometer, to diminish the influence of the installation errors. Finally, simulations and experiments are conducted to validate the correctness and effectiveness of proposed method. The results indicate that the optimization identification method proposed is effective and accurate.

Keywords Geometric errors · Translational axis · Laser interferometer · Installation errors · Sensitivity analysis

✉ Hongjian Xia
hjxia@gdut.edu.cn

[1] Guangdong Provincial Key Laboratory of Micro-nano Manufacturing Technology and Equipment, School of Electromechanical Engineering, Guangdong University of Technology, Guangzhou, Guangdong 510006, China

1 Introduction

As the requirement of precision machining has become higher in the field of aerospace, military industry, automobile and other industries, the performance of CNC machine tools is receiving increased attention in the manufacturing industry [1–3]. Translational axis is one of the most important components in multi-axis machine tools, to move the workpiece and the tool. Accuracy of translational axis directly affects the geometric accuracy of the CNC machine tool [4]. Measurement and identification of geometric errors of translational axis is the precondition for improving the geometric accuracy of CNC machine tools, especially for ultra-precision machine tools which need higher accuracy compensation. Therefore, an identification method of geometric errors of translational axis with high accuracy and insensitive to instrument installation errors is necessary [5].

Usually, the measurement method of geometric errors of translational axis can be classified into two categories: direct and indirect [6, 7]. Regarding direct measurement, errors are directly obtained by the measurement instruments without any auxiliary operations. Lee et al. [8] using a five-DOF measuring system and hybrid measurement technique to directly measure the geometric errors of machine tools with three translational axes. The positioning error of a translational axis is measured using a laser interferometer [9]. Laser diodes and beam splitters are applied for the measurement of three-axis machine tools [10]. In addition, some other newly designed measurement devices such as laser-based measuring systems and capacitance sensors were also utilized to measure geometric errors [11–13]. The above direct methods measure each error components step by step, therefore requires high-precision measuring instruments and trivial measurement procedures [14, 15]. However, the roll error in translational axis could not be measured directly using laser interferometer. In contrast to direct methods, the indirect methods are usually used to obtain the geometric errors from the identified model. The indirect method

generally identifies the geometric errors using less measurement paths than direct methods, and can identify all of error components of machine tools. Lots of research works have been completed regarding the indirect method [16–18]. Chen et al. [19] identified 21 geometric errors of three-axis machine tools using the 15 lines method. Measurement techniques were simplified by measuring the positioning errors along 15 lines in the machine workspace. However, the method is difficult and time-consuming to implement, requiring extensive computation. Wang et al. [20] used a laser tracking method to separate the geometric errors from the measured results in CNC milling machine based on the global positioning system (GPS) method. A multi-step identification method of error components was developed by using cross grid encoder measurement technology in a three-axis CNC vertical machining center [21]. Other commercial instruments like laser tracker, laser diode, and optics are also applied to measure geometric errors of translational axis [22–25]. Nevertheless, these laser tracker instruments have lower accuracy than laser interferometers and are time-consuming to operate, requiring highly skilled technicians.

The aforementioned studies mainly concerned how to identify geometric errors. Few research works have been conducted with considering the influence of instrument installation errors. The installation errors of instrument are inevitable and can affect the measurement result in the process of measurement. As for the indirect measurement method, the installation errors can make the measured result inaccuracy or even not trustworthy. However, in most of the studies, the installation position of the laser interferometer is only decided by the empirical during the measurement. These drawbacks can restrict the accuracy of error identification of translational axis, especially for precision detection in ultra-precision machine tools. For improving the robustness of identified approach of geometric errors, this paper proposes a measurement method which is insensitive to installation errors. Positioning errors and straightness errors of translational axis are measured through the laser interferometer with serial measurement paths. The corresponding identification model is built based on the least square method. During the measurement, a sensitivity analysis of identified matrix is also conducted to optimize measurement positions. Hence, a more precise identification procedure can be proposed to compute translational errors and rotational errors of translational axis from the measured results. The installation parameters of the measurement instrument are adjusted to minimize the influence of the installation errors. Finally, a range of simulations and experiments are conducted to verify the approach.

The structure of this paper is as follows. The geometric error modeling is described in detail in Section 2. Section 3 discusses the identification method of translational axis of geometric errors and Section 4 describes the sensitivity analysis of installation position errors. The simulation and experiment are conducted and their results are discussed in Section 5. Finally, the conclusions are drawn in Section 6.

2 The geometric errors modeling

2.1 Error parameter definition

According to reference [26], it is well known that when a component moves along an X-axis, it has six degrees of freedom. Its position description contains six errors accordingly which include three translational errors $\delta_x(X)$, $\delta_y(X)$, $\delta_z(X)$and three rotational errors$\varepsilon_x(X)$, $\varepsilon_y(X)$, $\varepsilon_z(X)$. Taking translational axis X as an example, these symbols of six error components are shown in Fig. 1.

2.2 Transformation matrix of adjacent bodies

The position and attitude of one body relative to another body could be expressed as the relative position and attitude of the coordinates system of adjacent body. The relationship between the platform and the base of the machine tool are shown in Fig. 2 which can be obtained by using the homogeneous transformation matrix. Figure 2 describes the motion relationship between the platform B_k and the adjacent base B_j. B_j carries the coordinate frame O_j and B_k is with coordinate frame O_k. Q_k is the motion reference frame of B_k in the initial position. During the relative motion between body B_j and B_k, kinematic components can contribute to the actual position and the attitude of body B_k involves ideal position offset P^l_{kh}, position errorP^e_{kh}, ideal motion amount $\mathbf{S}^l_{kh}$, and motion error amount$\mathbf{S}^e_{kh}$. P^l_{kh} and P^e_{kh} are combined into the actual position deviation P_{kh} between body B_k and B_j. $\mathbf{S}^l_{kh}$ and $\mathbf{S}^e_{kh}$ are combined into the actual motion amount $\mathbf{S}_{kh}$between body B_k and B_j; $\mathbf{r}_k$ refers to the position vector of the given point P (the laser measurement point) relative to O_k and $\mathbf{P}_{kp}$ is the position vector that the point P relative to Q_k.

In Fig. 2, the platform B_k moves relatively to B_j along the X-axis. Based on the theory of multi-body system [27–29]. The transformation matrix (${}^{\mathrm{j}}_{k}\mathbf{T}^{k}$) of the relative motion between B_k and B_j is obtained as follows:

$$ {}^{\mathrm{j}}_{k}\mathbf{T} = {}^{\mathrm{j}}_{k}\mathbf{T}\,{}^{\mathrm{j}}_{pk}\mathbf{T}\,{}^{\mathrm{j}}_{pek}\mathbf{T}\,{}^{\mathrm{j}}_{sk}\mathbf{T}\,{}^{\mathrm{j}}_{se} \tag{1} $$

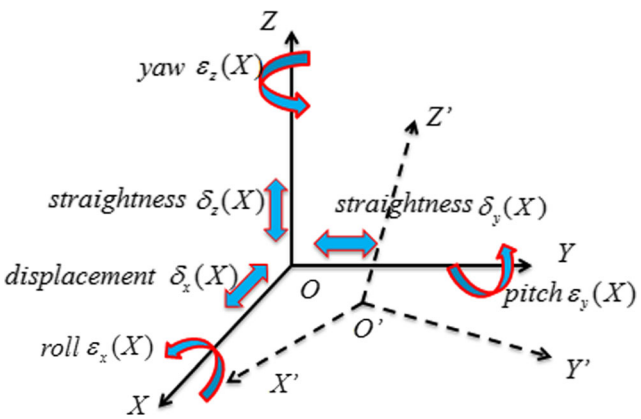

Fig. 1 Geometric error parameters of translational axis X

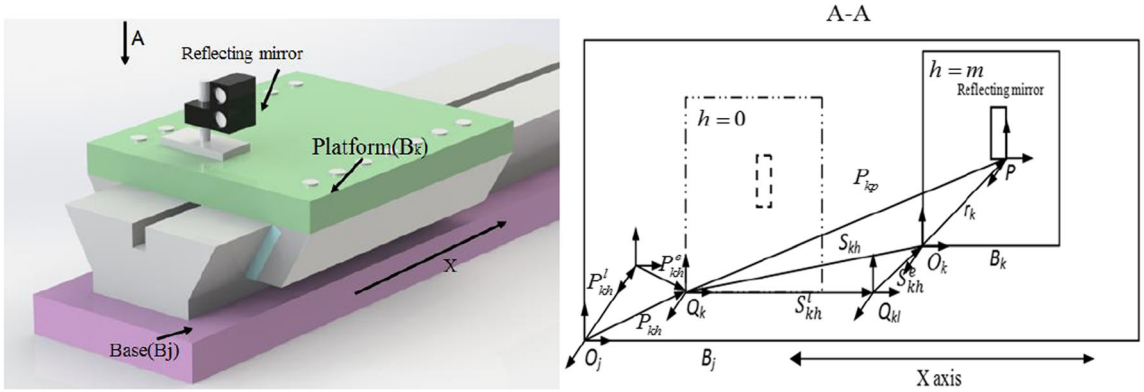

Fig. 2 Kinematic notations of linear axis

where, ${}^{\mathrm{j}}_{k}\mathbf{T}_{p}$ refers to the initiative position matrix between B_j and the motion reference frame, which denotes the initiative position of B_k;${}^{\mathrm{j}}_{k}\mathbf{T}_{pe}$ is the position error transformation matrix between B_j and B_k; ${}^{\mathrm{j}}_{k}\mathbf{T}_{s}$ is the motion transformation matrix between B_k and the motion reference frame, which denotes motion of B_k relative to the B_j; ${}^{\mathrm{j}}_{k}\mathbf{T}_{se}$ is the motion error transformation matrix between B_k and B_j:

$$ {}^{\mathrm{j}}_{k}\mathbf{T}_{p} = \begin{bmatrix} 1 & 0 & 0 & p^{\mathrm{l}}_{khx} \\ 0 & 1 & 0 & p^{l}_{khy} \\ 0 & 0 & 1 & p^{l}_{khz} \\ 0 & 0 & 0 & 1 \end{bmatrix} \tag{2} $$

In Eq.(2), P^{l}_{khx}, P^{l}_{khy}, and P^{l}_{khz} are the three linear position vectors of $\mathbf{P}^{l}_{kh}$ in the x, y, and z directions between coordinate systems of motion body B_j and B_k, respectively .

By the assumption of minor angles and ignoring the high-order deviations, the position error transformation matrix $({}^{\mathrm{j}}_{k}\mathbf{T}_{pe})$ is represented as follows:

$$ {}^{j}_{k}\mathbf{T}_{pe} = \begin{bmatrix} 1 & -\varepsilon^{khp}_{z} & \varepsilon^{khp}_{y} & p^{e}_{khx} \\ \varepsilon^{khp}_{z} & 1 & -\varepsilon^{khp}_{x} & p^{e}_{khy} \\ -\varepsilon^{khp}_{y} & \varepsilon^{khp}_{x} & 1 & p^{e}_{khz} \\ 0 & 0 & 0 & 1 \end{bmatrix} \tag{3} $$

where, P^{e}_{khx}, P^{e}_{khy}, and P^{e}_{khz} are the three linear position errors of $\mathbf{P}^{e}_{kh}$ in the x, y, and z directions between coordinate systems of motion body B_j and B_k, respectively;ε^{khp}_{x},ε^{khp}_{y} andε^{khp}_{z} are three rotational errors in *x-*, *y-*, and *z- axes* between coordinate systems of body B_k and B_j.

The motion transformation matrix $({}^{\mathrm{j}}_{k}T_{s})$is defined as follows:

$$ {}^{\mathrm{j}}_{k}T_{s} = \begin{bmatrix} 1 & 0 & 0 & \delta^{l}_{khx} \\ 0 & 1 & 0 & \delta^{l}_{khy} \\ 0 & 0 & 1 & \delta^{l}_{khz} \\ 0 & 0 & 0 & 1 \end{bmatrix} \tag{4} $$

In which, δ^{l}_{khx}, δ^{l}_{khy}, and δ^{l}_{khz} are the three linear motion vectors of the $\mathbf{S}^{l}_{kh}$ in the x, y, and z directions between coordinate systems of motion body B_j and B_k, respectively .

The motion error transformation matrix $({}^{\mathrm{j}}_{k}\mathbf{T}_{se})$ is follows:

$$ {}^{\mathrm{j}}_{k}T_{se} = \begin{bmatrix} 1 & -\varepsilon^{khs}_{z}(x) & \varepsilon^{khs}_{y}(x) & \delta^{e}_{khx} \\ \varepsilon^{khs}_{z}(x) & 1 & -\varepsilon^{khs}_{x}(x) & \delta^{e}_{khy} \\ -\varepsilon^{khs}_{y}(x) & \varepsilon^{khs}_{x}(x) & 1 & \delta^{e}_{khz} \\ 0 & 0 & 0 & 1 \end{bmatrix} \tag{5} $$

where, δ^{e}_{khx}, δ^{e}_{khy}, and δ^{e}_{khz} are the three linear motion errors of the $\mathbf{S}^{e}_{kh}$ in the x, y, and z directions between coordinate systems of motion body B_j and B_k, respectively;$\varepsilon^{khs}_{x}(x)$, $\varepsilon^{khs}_{y}(x)$, and $\varepsilon^{khs}_{z}(x)$ are the rotational motion errors of kinematics pair.

Assume that the coordinates of B_k is coincide with B_j at the beginning when the platform B_k moves along the *X*-axis. The relative position equation of the measurement point P moves along the *X*-axis. Therefore, it can be deduced as follows:

$$ \begin{bmatrix} p_{kp} \\ 1 \end{bmatrix} = {}^{\mathrm{j}}_{k}T^{k}\begin{bmatrix} r_k \\ 1 \end{bmatrix} = {}^{\mathrm{j}}_{k}T^{k}\,{}^{\mathrm{j}}_{sk}T^{k}\,{}_{se}\begin{bmatrix} r_k \\ 1 \end{bmatrix} \tag{6} $$

Referring to Eqs.(4) and (5), Eq.(6) can be represented as follows:

$$ \begin{bmatrix} x_{kh} \\ y_{kh} \\ z_{kh} \\ 1 \end{bmatrix} = \begin{bmatrix} 1 & 0 & 0 & \delta^{l}_{khx} \\ 0 & 1 & 0 & \delta^{l}_{khy} \\ 0 & 0 & 1 & \delta^{l}_{khz} \\ 0 & 0 & 0 & 1 \end{bmatrix} \begin{bmatrix} 1 & -\varepsilon^{khs}_{z}(x) & \varepsilon^{khs}_{y}(x) & \delta^{e}_{khx} \\ \varepsilon^{khs}_{z}(x) & 1 & -\varepsilon^{khs}_{x}(x) & \delta^{e}_{khy} \\ -\varepsilon^{khs}_{y}(x) & \varepsilon^{khs}_{x}(x) & 1 & \delta^{e}_{khz} \\ 0 & 0 & 0 & 1 \end{bmatrix} \begin{bmatrix} X_k \\ Y_k \\ Z_k \\ 1 \end{bmatrix} \tag{7} $$

In which, x_{kh}, y_{kh}, and z_{kh} are the vector components of $\mathbf{p}_{kp}$ in the x, y, and z directions between coordinate systems of Q_k and measurement point P; X_k, Y_k,and Z_k are the vector components of $\mathbf{r}_k$in the x, y, and z directions between coordinate systems of O_k and measurement point P.

Eq.(7) can be rewritten as follows:

$$\begin{bmatrix} x_{kh} \\ y_{kh} \\ z_{kh} \end{bmatrix} = \begin{bmatrix} \delta^l_{khx} \\ \delta^l_{khy} \\ \delta^l_{khz} \end{bmatrix} + \begin{bmatrix} \delta^e_{khx} \\ \delta^e_{khy} \\ \delta^e_{khz} \end{bmatrix} + \begin{bmatrix} 1 & -\varepsilon^{khs}_z(x) & \varepsilon^{khs}_y(x) \\ \varepsilon^{khs}_z(x) & 1 & -\varepsilon^{khs}_x(x) \\ -\varepsilon^{khs}_y(x) & \varepsilon^{khs}_x(x) & 1 \end{bmatrix} \begin{bmatrix} X_k \\ Y_k \\ Z_k \end{bmatrix} \tag{8}$$

When the platform B_k locates in the initial position ($h = 0$) shown in Fig. 2, Eq.(8) can be expressed as follows:

$$\begin{bmatrix} x_{k0} \\ y_{k0} \\ z_{k0} \end{bmatrix} = \begin{bmatrix} \delta^l_{k0x} \\ \delta^l_{k0y} \\ \delta^l_{k0z} \end{bmatrix} + \begin{bmatrix} \delta^e_{k0x} \\ \delta^e_{k0y} \\ \delta^e_{koz} \end{bmatrix} + \begin{bmatrix} 1 & -\varepsilon^{k0s}_z(x) & \varepsilon^{k0s}_y(x) \\ \varepsilon^{k0s}_z(x) & 1 & -\varepsilon^{k0s}_x(x) \\ -\varepsilon^{k0s}_y(x) & \varepsilon^{k0s}_x(x) & 1 \end{bmatrix} \begin{bmatrix} X_k \\ Y_k \\ Z_k \end{bmatrix} \tag{9}$$

When the measurement point P moves from the initial position to the position m ($h = m$) shown in Fig. 2, the displacement between the position m and the initial position is:

$$\begin{bmatrix} x_{km}-x_{k0} \\ y_{km}-y_{k0} \\ z_{km}-z_{k0} \end{bmatrix} = \begin{bmatrix} \delta^l_{kmx}-\delta^l_{k0x} \\ \delta^l_{kmy}-\delta^l_{k0y} \\ \delta^l_{kmz}-\delta^l_{k0z} \end{bmatrix} + \begin{bmatrix} \delta^e_{kmx}-\delta^e_{k0x} \\ \delta^e_{kmy}-\delta^e_{koy} \\ \delta^e_{kmz}-\delta^e_{k0z} \end{bmatrix}$$

$$+ \begin{bmatrix} 0 & -\varepsilon^{kms}_z(x)+\varepsilon^{k0s}_z(x) & \varepsilon^{kms}_y(x)-\varepsilon^{k0s}_y(x) \\ \varepsilon^{kms}_z(x)-\varepsilon^{k0s}_z(x) & 0 & -\varepsilon^{kms}_x(x)+\varepsilon^{k0s}_x(x) \\ -\varepsilon^{kms}_y(x)+\varepsilon^{k0s}_y(x) & \varepsilon^{kms}_x(x)-\varepsilon^{k0s}_x(x) & 0 \end{bmatrix} \begin{bmatrix} X_k \\ Y_k \\ Z_k \end{bmatrix} \tag{10}$$

Assume that O_k are coincide with Q_k in the initial position and there are no error in the initial position, the error components($\delta^l_{k0x}, \delta^l_{k0y}, \delta^l_{k0z}, \delta^e_{k0x}, \delta^e_{k0y}, \delta^e_{k0z}, \varepsilon^{k0s}_x(x)$, $\varepsilon^{k0s}_y(x), \varepsilon^{k0s}_z(x)$) in Eq.(9) are equal to zero when B_k is set in the initial position ($h = 0$). Therefore, the displacement can be simplified as:

$$\begin{bmatrix} x_{km} & -x_{k0} & -\delta^l_{kmx} \\ y_{km} & -y_{k0} & -\delta^l_{kmy} \\ z_{km} & -z_{k0} & -\delta^l_{kmz} \end{bmatrix} = \begin{bmatrix} \delta^e_{kmx} \\ \delta^e_{kmy} \\ \delta^e_{kmz} \end{bmatrix} + \begin{bmatrix} 0 & -\varepsilon^{kms}_z(x) & \varepsilon^{kms}_y(x) \\ \varepsilon^{kms}_z(x) & 0 & -\varepsilon^{kms}_x(x) \\ -\varepsilon^{kms}_y(x) & \varepsilon^{kms}_x(x) & 0 \end{bmatrix} \begin{bmatrix} X_k \\ Y_k \\ Z_k \end{bmatrix} \tag{11}$$

Eq.(11) can be rewritten as:

$$\begin{bmatrix} x_{km}-x_{k0}-\delta^l_{kmx} \\ y_{km}-y_{k0}-\delta^l_{kmy} \\ z_{km}-z_{k0}-\delta^l_{kmz} \end{bmatrix} = \begin{bmatrix} 0 & -\varepsilon^{kms}_z(x) & \varepsilon^{kms}_y(x) & \delta^e_{kmx} \\ \varepsilon^{kms}_z(x) & 0 & -\varepsilon^{kms}_x(x) & \delta^e_{kmy} \\ -\varepsilon^{kms}_y(x) & \varepsilon^{kms}_x(x) & 0 & \delta^e_{kmz} \\ 0 & 0 & 0 & 1 \end{bmatrix} \begin{bmatrix} X_k \\ Y_k \\ Z_k \\ 1 \end{bmatrix} \tag{12}$$

From Eq.(12), it is obvious that three or more equations are needed to solve the six geometric errors of X-axis.

3 The geometric error identification of translational axis

In this paper, a redundancy measurement approach to identify geometric errors of a translational axis is proposed. The measurement paths for translational X-axis are shown in Fig. 3. There are four measurement paths for translational axis, and only one single translational axis is controlled during the measurement in order to get the laser interferometer data. Four installation position $P_1(X_1,Y_1,Z_1)$, $P_2(X_2,Y_2,Z_2)$, $P_3(X_3,Y_3,Z_3)$, and $P_4(X_4,Y_4,Z_4)$ are selected and installed in the workbench as can be seem in Fig. 3. The distance between the P_1 and P_2 is H in the Z direction. The distance between P_3 and P_1 is W in the Y direction. The distance between P_4 and P_3 is H in the Z direction. Measure points(n_1,…, n_i) are equally distributed on the translational X-axis stroke. In the process of measurement, comprehensive errors of mounting point P_i, including positioning errors in X direction and two straightness errors in $Y$and Z direction, would be measured in every measure points(n_1,…, n_i), respectively. After the measurement of installation point P_i being completed, other installation point would be selected to be measured following the same steps mentioned above until all of installation points have been tested.

On each measurement Line(Line1, Line2, Line3, and Line4), positioning errors ($\Delta x_i(X)$), and straightness errors($\Delta y_i(X)$, $\Delta z_i(X)$) on each installation position are measured by the laser interferometer. $\Delta x_i(X)$ are the positioning errors of the Line i along X-axis direction. $\Delta y_i(X)$ refers to the straightness errors of Line i along X-axis in Y-axis direction. $\Delta z_i(X)$ is the straightness error of the line i along X-axis in Z direction. Then, the identification model can be constructed according to the 12 measured results[$\Delta x_1(X)$ $\Delta y_1(X)$ $\Delta z_1(X)$ $\Delta x_2(X)$ $\Delta y_2(X)$ $\Delta z_2(X)$ $\Delta x_3(X)$ $\Delta y_3(X)$ $\Delta z_3(X)$ $\Delta x_4(X)$ $\Delta y_4(X)$ $\Delta z_4(X)$] and the six error items [$\delta_X(X)$ $\delta_Y(X)$ $\delta_Z(X)$ $\varepsilon_X(X)$ $\varepsilon_Y(X)$ $\varepsilon_Z(X)$].The position of installation point P_i could be expressed as r_{p_i}, where $r_{p_i} = [X_i \quad Y_i \quad Z_i]^T$.

From Eq.(12), the relationship between comprehensive errors measured by laser interferometer and geometric error parameters of machine tool can be deduced:

$$\begin{bmatrix} x_{km}-x_{k0}-\delta^l_{kmx} \\ y_{km}-y_{k0}-\delta^l_{kmy} \\ z_{km}-z_{k0}-\delta^l_{kmz} \end{bmatrix} = \begin{bmatrix} \Delta x_i(X) \\ \Delta y_i(X) \\ \Delta z_i(X) \end{bmatrix} \tag{13}$$

Referring to Eqs.(12) and (13), Eq.(14) can be represented as follows:

$$\Delta P_i(X) = \begin{pmatrix} I_3 & -[r_{P_i}\times] \end{pmatrix} \begin{bmatrix} \delta(X) \\ \varepsilon(X) \end{bmatrix} \quad i = 1,2,3,4 \tag{14}$$

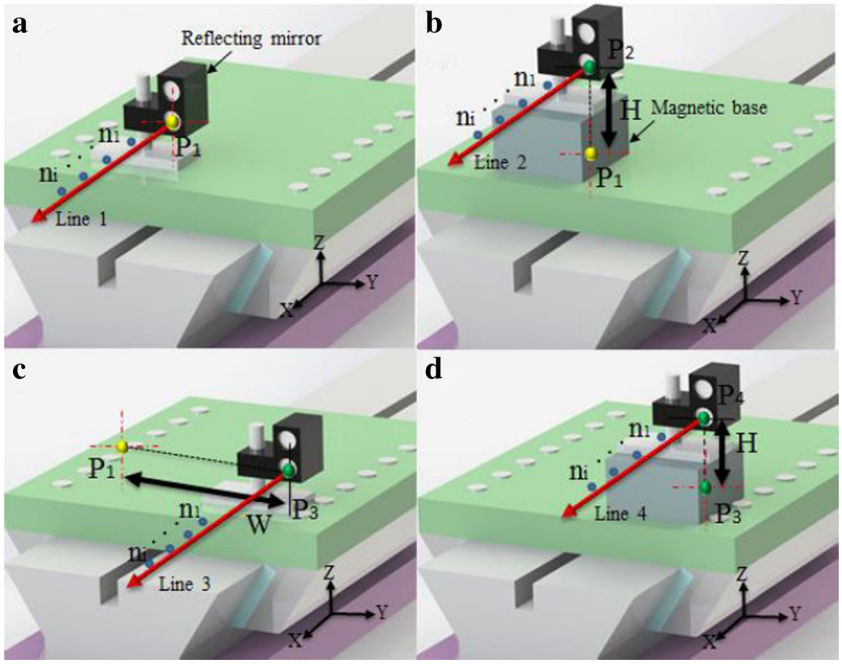

Fig. 3 Measurement paths for the geometric errors of the translational axis. **a** First measurement. **b** Second measurement. **c** Third measurement. **d** Fourth measurement

In which, $\Delta P_i(X)$ refers to the position error vector of installation point P_i, $\{\Delta P_i(X)\} = [\Delta x_i(X) \ \Delta y_i(X) \ \Delta z_i(X)]^T$; I_3 is identity matrix; $[r_{P_i}\times]$ is antisymmetric matrix of vector r_{p_i}, $[r_{P_i}\times] = \begin{bmatrix} 0 & -Z_i & Y_i \\ Z_i & 0 & -X_i \\ -Y_i & X_i & 0 \end{bmatrix}$; $\{\delta(X)\} = [\delta_X(X) \ \ \delta_Y(X) \ \ \delta_Z(X)]^T$; $\{\varepsilon(X)\} = [\varepsilon_X(X) \ \varepsilon_Y(X) \ \varepsilon_Z(X)]^T$.

Positioning errors and two straightness errors on each installation position are measured by the laser interferometer. The mathematical model could be deduced by 12 measurement results from Eq. (15).

$$\{\Delta(X)\} = [E_x]\begin{bmatrix}\delta(X)\\ \varepsilon(X)\end{bmatrix} \tag{15}$$

In which, $\Delta(X)$ refer to comprehensive errors of four installation point P_i, $\{\Delta(X)\} = [\Delta P_1(X) \ \Delta P_2(X) \ \Delta P_3(X) \ \Delta P_4(X)]^T$;

$$[\mathbf{E}_x] = \begin{bmatrix} I_3 & -[r_{P_1}\times] \\ I_3 & -[r_{P_2}\times] \\ I_3 & -[r_{P_3}\times] \\ I_3 & -[r_{P_4}\times] \end{bmatrix} \tag{16}$$

It has been found that they are over determined systems from Eq. (15). In order to calculate their solution, both sides should be multiplied with $[\mathbf{E}_x]^T$.

$$[E_x]^T\{\Delta(X)\} = [E_x]^T[E_x]\begin{bmatrix}\delta(X)\\ \varepsilon(X)\end{bmatrix} \tag{17}$$

The least square solution for the six geometric error items is then applied by using the pseudo invert matrix.

$$\begin{bmatrix}\delta(X)\\ \varepsilon(X)\end{bmatrix} = \left([E_x]^T[E_x]\right)^{-1}[E_x]^T\{\Delta(X)\} \tag{18}$$

In Eq. (18), the selection of the coordinates (X_1, Y_1, Z_1), (X_2, Y_2, Z_2), (X_3, Y_3, Z_3), and (X_4, Y_4, Z_4) should be able to ensure that the coefficient of $([E_x]^T[E_x])^{-1}$ matrix is nonsingular to achieve an unique solution and to be identified as the error items ($\delta_x(X)$, $\delta_y(X)$,$\delta_z(X)$, $\varepsilon_x(X)$, $\varepsilon_y(X)$, and $\varepsilon_z(X)$). In this condition, the geometric errors of translational axis on a five-axis machine tool could be identified. Redundancy measurement method through increasing measurement parameters to obtain more information can make the identified results more reliable and stable, which have been applied in many fields [30, 31]. The geometric error identification method proposed in this article makes the identified results more reliable and stable by increasing measurement parameters of comprehensive errors on a translational axis, which can reduce the influence of accidental factors on the measurement. To a certain extent, the measurement result from above method can reflect the characteristics of the machine tool accuracy because the measurement coordinate was selected in the machine tool working space.

As shown in Eq. (18), redundancy measurement identification approach is expressed as the function of the position coordinates of the measuring point P, the values of the comprehensive measurement errors and the six geometric errors of one single axis. To ensure that Eq. (18) can be solved, the matrix $([E_x]^T[E_x])^{-1}$ must be nonsingular; thus, the installation

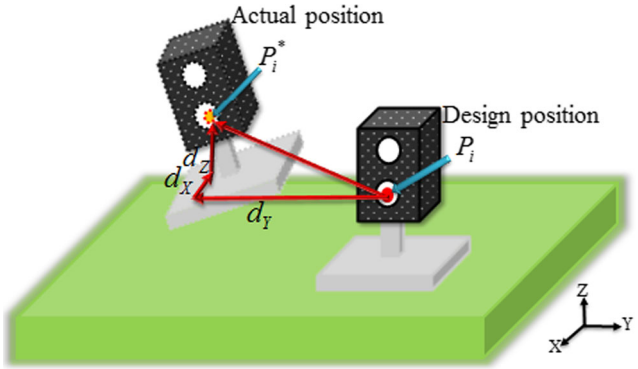

Fig. 4 The effect of installation position errors

parameters W and H have to satisfy the conditions $W \neq 0$ and $H \neq 0$. Furthermore, the values of H and W should have significant effect on the solution of Eq. (18). Therefore, the further analysis of the influence of the parameters of H and W will be conducted. A method based on the sensitivity analysis of matrix $([E_x]^T[E_x])^{-1}$ is proposed to find the optimal installation parameters for the measurement system in order to identify the error items more precisely.

4 Sensitivity analysis and optimization

The proposed method could effectively identify the geometric errors of translational axis. However, the identified result obtained from the above approach is influenced by the installation errors in some cases. Thus, in order to improve the measurement accuracy, it is necessary to further analyze the influence of the position error. Assuming that the position of ideal installation point P_i has slight offset (d_X, d_Y, d_Z exaggeration shown in Fig. 4) from actual installation point P_i^*. From Eq. (16), due to the existence of the position errors, there are offset existing between actual parameters and preset parameters of (H, W). The identification result of six geometric errors which derived from the inaccuracy of the measured results and the installation parameters (H, W) would be affected. Therefore, in this study, a mathematical model for the position error sensitivity analysis is developed to provide a theoretical basis for the suitable measuring position selection.

Referring to Eq. (18), let $E_x^* = ([E_x]^T[E_x])$, $X = [\delta(X)\ \varepsilon(X)]$ and $B = [E_x]^T\{\Delta(X)\}$. The redundancy measurement identification model is represented as follows:

$$X = (E_x*)^{-1}B \tag{19}$$

From Eq. (16), the installation errors will result in the perturbation in the coefficient matrix E_x^*which can be expressed as δ_{E_x*}. The inaccuracy of the measurement system can also cause the disturbance in vector B which can be represented by δ_B. Therefore,δ_{E_x*} and δ_B will result in the change δ_X of the solution. The relationship between disturbance and their correspondence matrix can be shown below:

$$(X + \delta_X)\left(E_x^* + \delta_{E_x*}\right) = (B + \delta_B) \tag{20}$$

The change rate of the solution can be expressed by the inequality in norm form according to the literature [32].

$$\frac{\|\delta_X\|}{\|X\|} \leq \frac{\left\|(E_x*)^{-1}\right\|\left\|E_x^*\right\|}{1-\left\|(E_x*)^{-1}\right\|\left\|E_x^*\right\|\frac{\|\delta_{E_x*}\|}{\|E_x^*\|}}\left(\frac{\|\delta_B\|}{\|B\|}+\frac{\|\delta_{E_x*}\|}{\|E_x\|}\right) \tag{21}$$

The norm of coefficient matrix $\|(E_x*)^{-1}\|\|E_x^*\|$ reflects the sensitivity of the solution of equations with respect to original

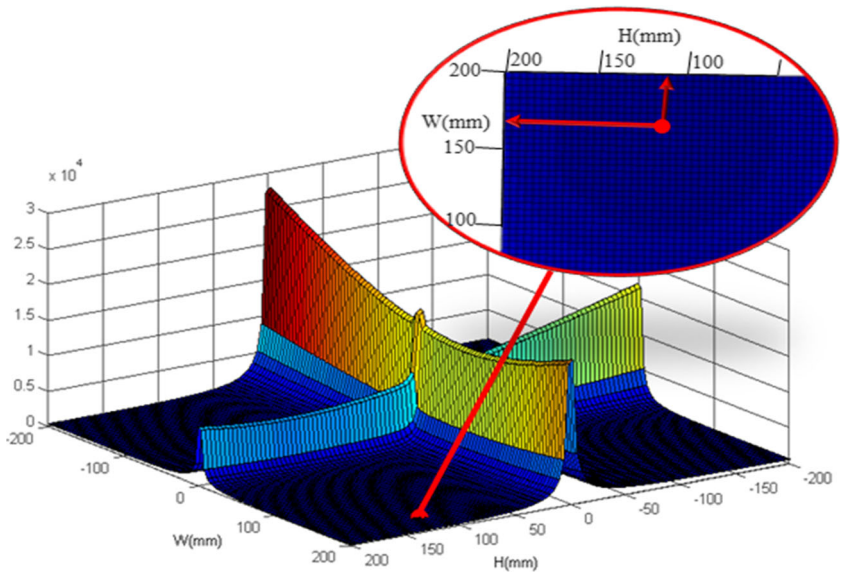

Fig. 5 Simulation results for the condition number according to the changing with the value (H, W)

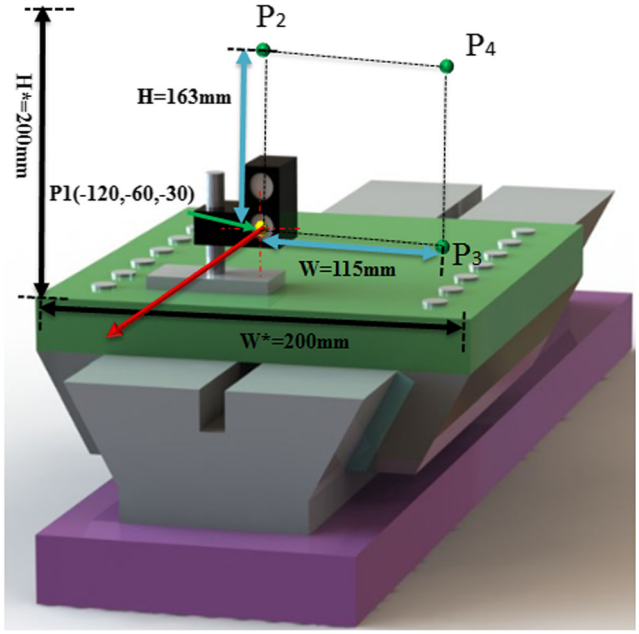

Fig. 6 Optimum installation parameters in machine tool

data errors. Theoretically speaking, it is also called condition number. To simplify the calculation, the two norm is selected to represent the condition number of the coefficient matrix E_x^*.

$$cond\left(E_x^*\right) = \left\|(E_x*)^{-1}\right\|_2 \left\|E_x^*\right\|_2 \tag{22}$$

From Eq. (22), the condition number $cond(E_x^*)$is determined by the installation parameters (H, W). The parameter H and W respectively depends on the height and the width of the reflecting mirror relatively to the position of the first measurement point. In order to obtain better measurement to the machine tool, the first measurement point is usually chosen on the position where machine tool processing frequently. Therefore, selecting a proper value for parameter (H, W) to minimize the condition number $cond(E_x^*)$ can diminish the influence of the errors of the solution derived from the inaccuracy of the measured results and the installation location. Then, the optimization task is represented by $\min(\|(E_x*)^{-1}\|_2\|E_x^*\|_2)|_{H,W}$.

A program has been developed to evaluate the condition number changing with the value (H, W) at the different position of the translational axis (first measurement point was set at ($X_1 = -120$, $Y_1 = -60$, $Z_1 = -30$)).

As shown in Fig. 5, the condition number decreases rapidly when the value of H increases before about 115 mm in positive direction and W increases before about 163 mm in positive direction. After that, it increases again. Thus, there is an optimum value of W and H (shown in Fig. 6 (H = 115 mm, W = 163 mm)) that the minimum condition number can be achieved at the first measurement point ($X_1 = -120$, $Y_1 = -60$, $Z_1 = -30$) in the range of W* and H* between 0 and 200 mm.

Obviously, there has different optimum value (H, W) at the different first measurement point. In engineering practice, first measurement point is usually selected on the position where machine tool processing frequently in order to obtain better compensation results. Once the first measurement point have been chosen at the machine work zone, then the optimum value (H, W) are selected as the installation parameter.

In this paper, a redundancy measurement approach is proposed. By increasing measurement parameters, more information can be obtained. The accuracy of identified results is improved through redundancy measurement method. To a certain extent, the method diminishes the influence of installation errors. However, the installation errors still exist in the method. Sensitivity analysis was conducted to improve the measurement accuracy. Through sensitivity analysis,

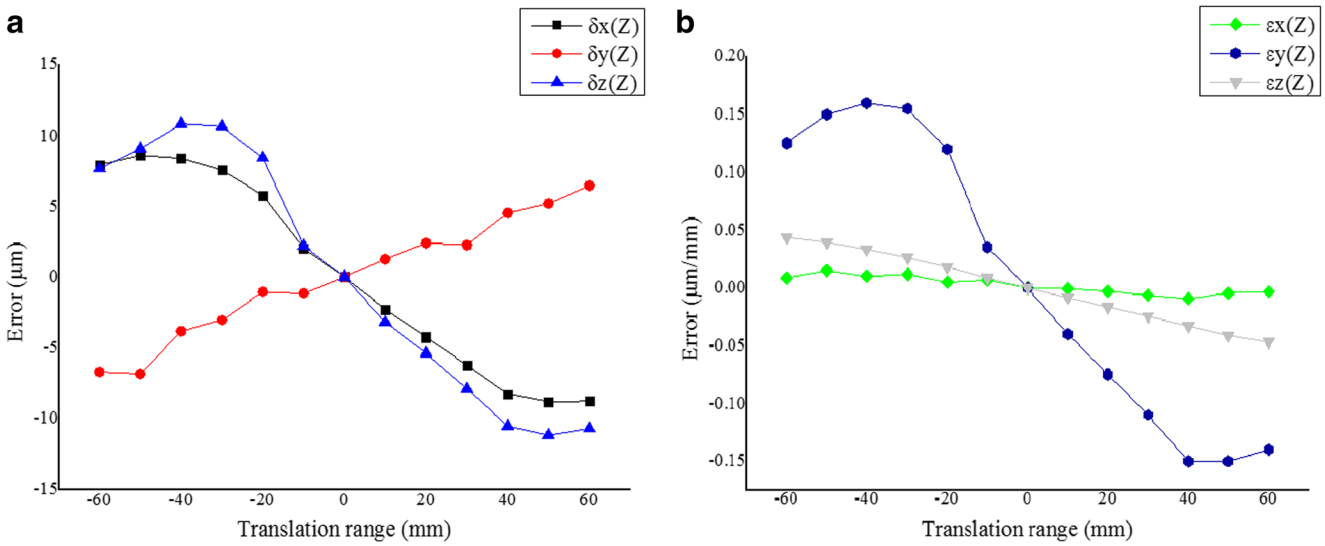

Fig. 7 Six geometric errors of translational axis Z. **a** Three translational errors. **b** Three rotational errors

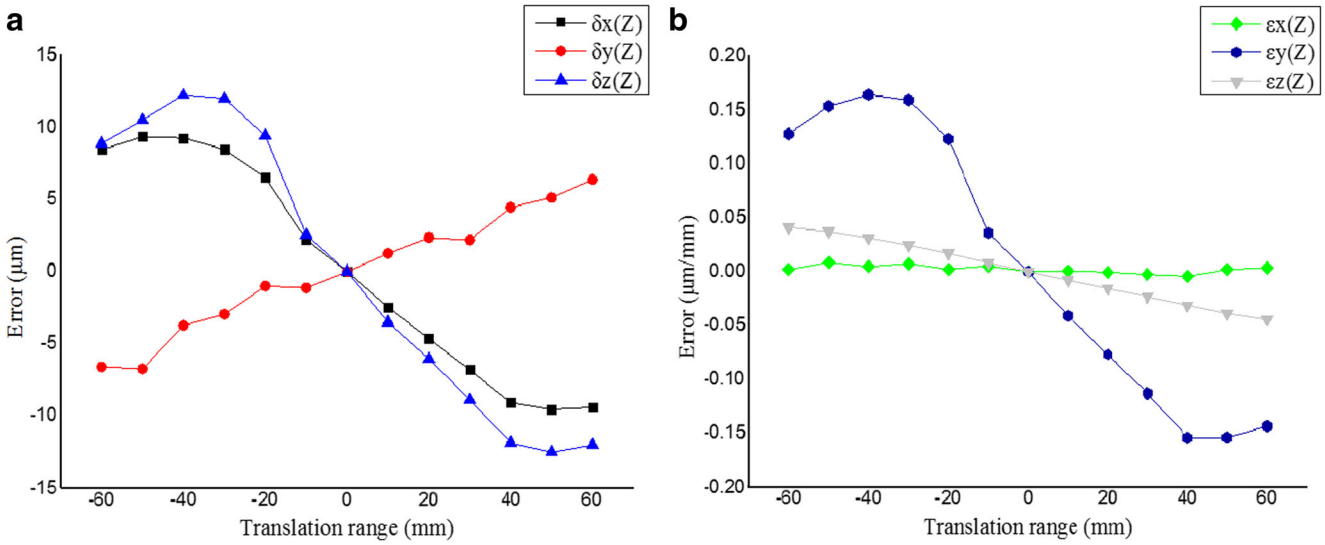

Fig. 8 The six geometric errors of translational axis *Z* computing by r edundancy measurement method. **a** Three translational errors. **b** Three rotational errors

optimum installation position, which was not sensitive to the influence of the position errors, has been chosen. The influence of installation errors could be decrease rapidly through the method when measuring in the optimum positions. Simulations and experiments are conducted to validate the effectiveness of the proposed method.

5 Simulation and experimental verification

5.1 Simulation example

Simulation was used to validate the effectiveness of measurement method proposed in this article. Two measurement strategies using redundancy measurement and redundancy measurement with sensitivity analysis are applied to validate their effectiveness. Redundancy measurement is the method that is conducted measurement in random positions, while the redundancy measurement with sensitivity analysis is the method that is measured in the optimum positions. The simulation strategy consists of three steps is designed as follows: (1) the six geometric errors of translational axis *Z* and set-up errors of reflecting mirror were generated; (2) the six geometric errors of translational axis Z were identified through redundancy measurement method and redundancy measurement method with sensitivity analysis respectively; (3) two measurement methods were applied to estimate positioning error of *Z*-axis, and the result of positioning error deviation between generated and estimated were compared. The generated six geometric errors of translational axis *Z* are shown in Fig. 7.

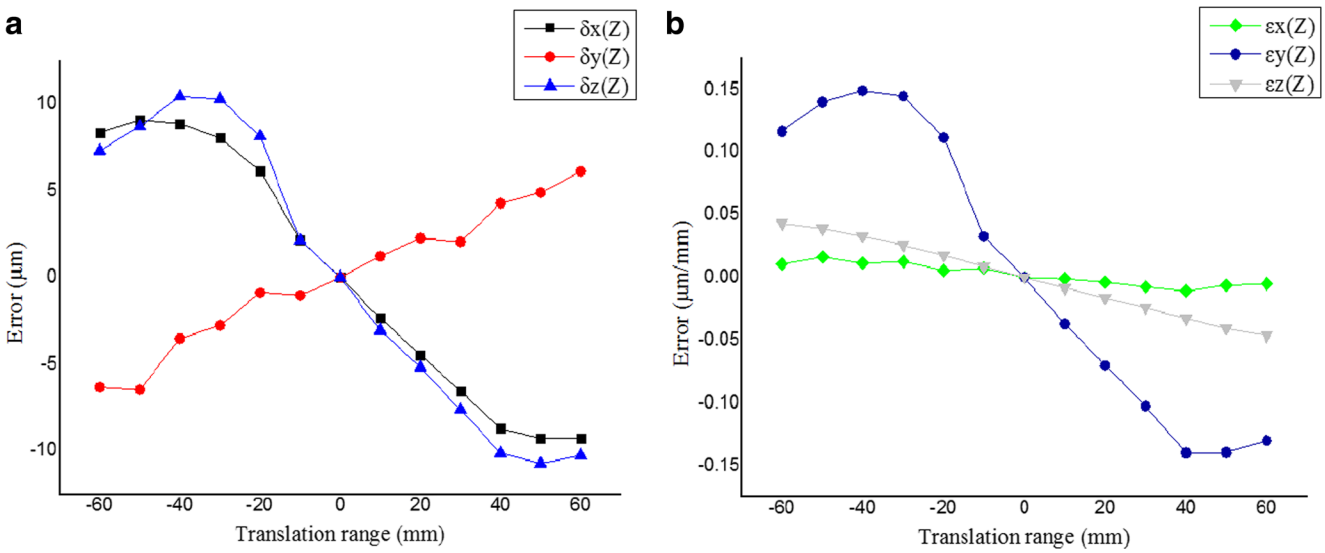

Fig. 9 The six geometric errors of translational axis *Z* computing by redundancy measurement method with sensitivity analysis. **a** Three translational errors. **b** Three rotational errors

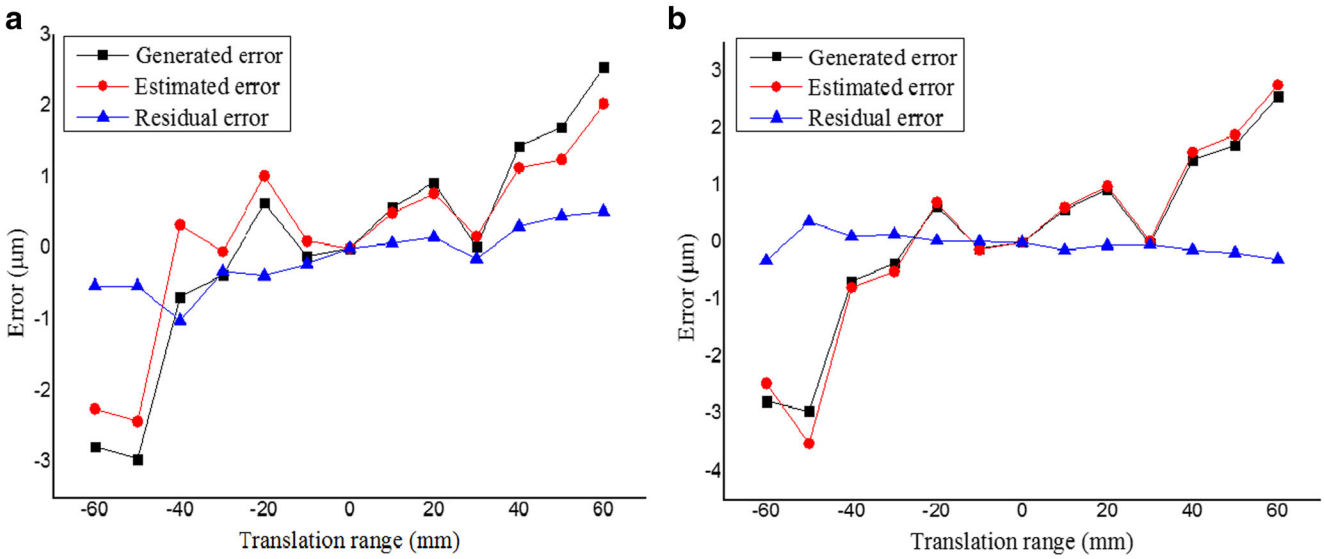

Fig. 10 Deviation between generated and estimated errors. **a** The estimated errors computing by redundancy measurement method. **b** The estimated errors computing by redundancy measurement method with sensitivity analysis

The simulation parameters are listed in Table. 1. Set-up error ($\Delta x_i = \pm 3$, $\Delta y_i = \pm 3$, $\Delta z = \pm 3_i$, mm) are applied to each installation position of reflecting mirror using Eq. 16 through two measurement strategies. As can be seen in Fig. 8, the six geometric errors of translational axis Z were identified using redundancy measurement method. The six geometric errors of translational axis Z were identified using redundancy measurement method with sensitivity analysis as shown in Fig. 9. Results of positioning error deviation between generated and estimated using two measurement method were shown in Fig. 10.

Figures 8 and 9 show the translational and rotational error components identified by redundancy measurement method and redundancy measurement method with sensitivity analysis respectively. According to the curves in Figs. 8 and 9, the curves of geometric errors, which identified by both measurement method, are approximately coincide with the curves of geometric errors, generated in Fig. 7. The main difference between Figs. 8 and 9 are the curves of $\delta_z(Z)$ and $\varepsilon_y(Z)$. The curves of $\delta_z(Z)$ and $\varepsilon_y(Z)$ in Fig. 9 are more coincide with the curves of geometric errors generated in Fig. 7 than in Fig. 8. $\delta_z(Z)$ and $\varepsilon_y(Z)$ play an important role in the positioning error of axis Z. After identifying six geometric errors of translational axis Z through both measurement methods, the positioning error of axis Z has been calculated using Eq. 15 and the result is shown in Fig. 10. Referring to Fig. 10, the generated error means the positioning error of Z-axis, which is calculated through the generated geometric errors. The estimated errors expressed the positioning error of axis Z, which is calculated through the identified geometric errors in Figs. 8 and 9,

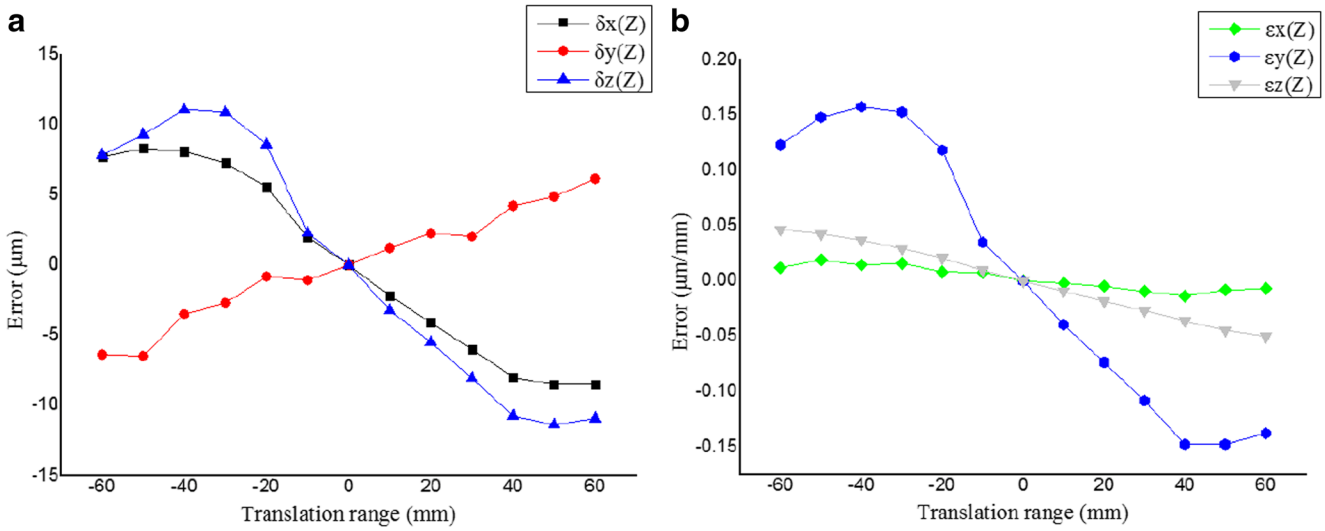

Fig. 11 The six geometric errors of translational axis Z computing by the general non-collinear three measurement lines method. **a** Three translational errors. **b** Three rotational errors

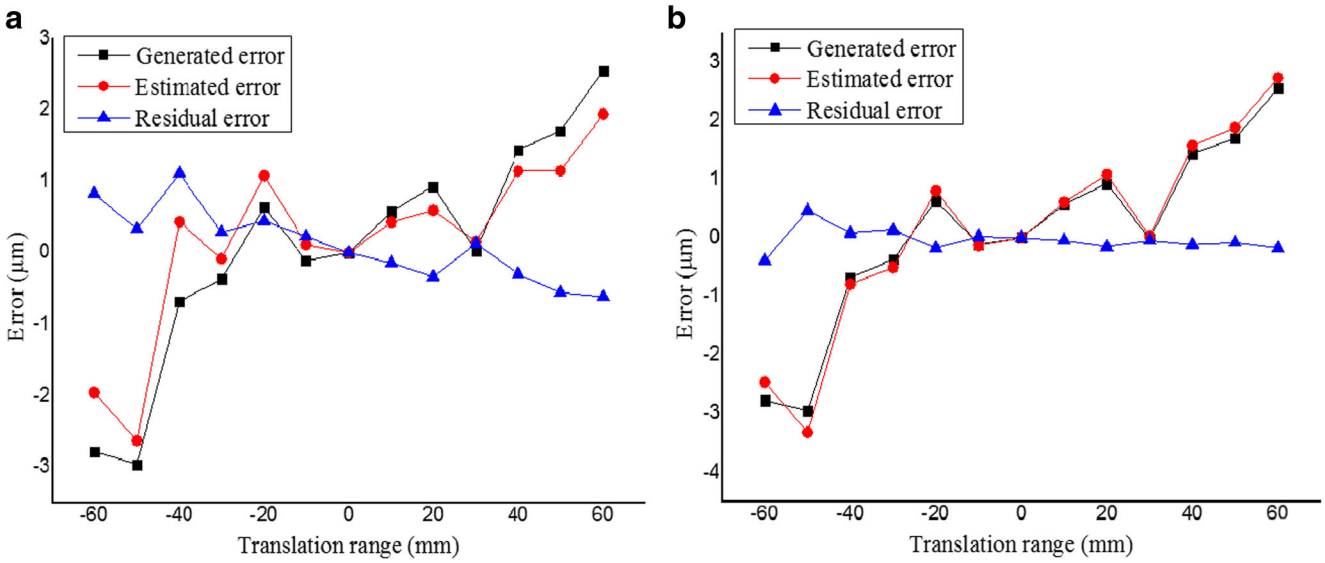

Fig. 12 Deviation between generated and estimated errors. **a** The estimated errors computing by the general non-collinear three measurement lines method. **b** The estimated errors computing by redundancy measurement method with sensitivity analysis

respectively. The residual error means the difference between generated error and estimated error. The residual errors of two methods are smaller when it gets close to the origin. On the contrary, when it is far away from the origin, the curve of estimated errors does not fit well with the curve of generated errors (discrepancies within 1 μm with redundancy measurement method). This is because, small estimate deviation of rotational errors including (pitch, yaw, and roll) due to the long distance would cause a large magnitude of positioning error of axis *Z*. Compared with the result of positioning error deviation between generated and estimated for two measurement methods, the curve of estimated error identified by the redundancy measurement method with sensitivity analysis (discrepancies within 0.5 μm) are closer to the generated curve than the one identified by the redundancy measurement method (discrepancies within 1 μm). Since the residual errors are in acceptable levels, the usefulness of the proposed method can be shown.

To further validate the proposed method, other comparative simulations are conducted to estimate the positioning error of translational axis *Z*. Three non-collinear measurement points $P_0(-118, -60, -30)$, $Q_0(-60, 70, -23)$, and $K_0(-20, -10, -39)$ are selected according to the general non-collinear three measurement lines method [25]. Set-up errors ($\Delta x_i = \pm 1$, $\Delta y_i = \pm 2$, $\Delta z_i = \pm 3$, mm) are applied to each measurement position through two measurement strategies. The six geometric errors of translational axis *Z* (shown in Fig. 11) were identified by using methods presented in the literature [25]. As shown in

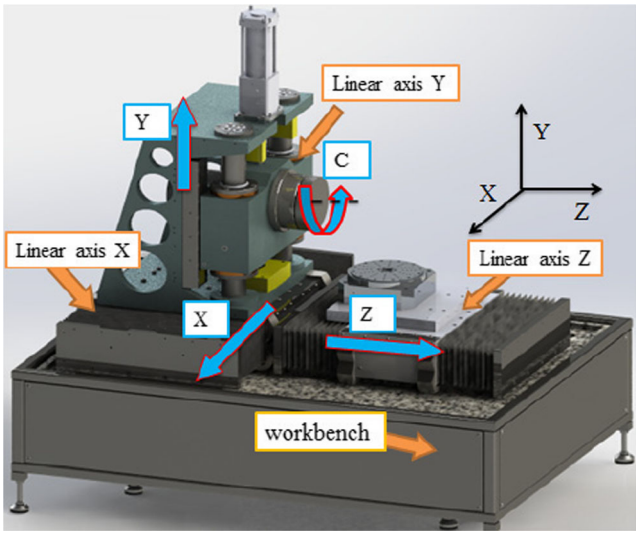

Fig. 13 Machine tool structure

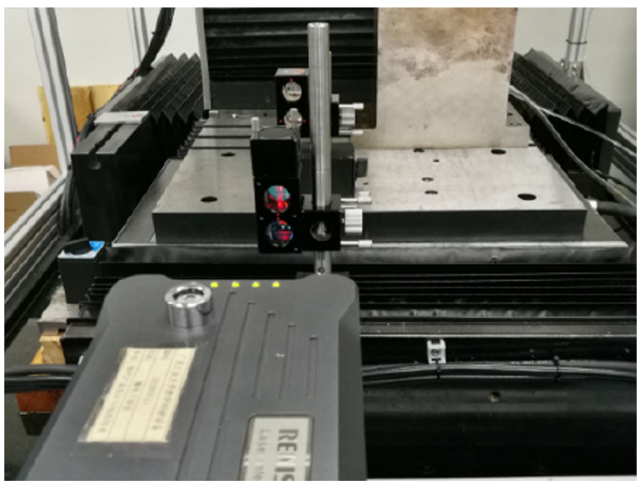

Fig. 14 Measurement at the four-axis machining center

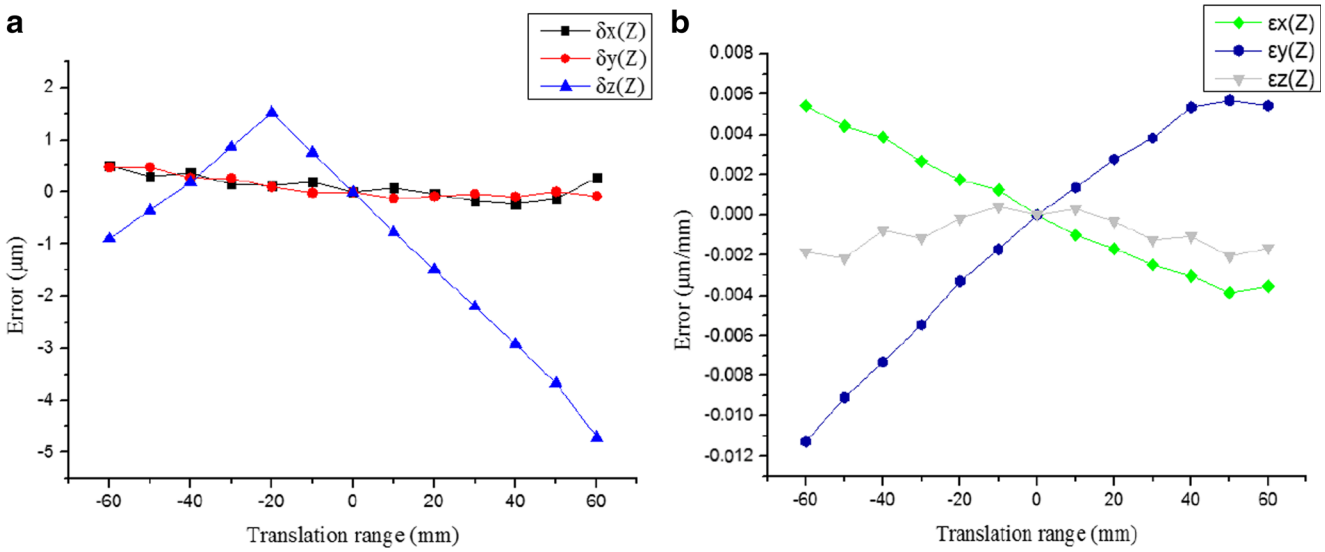

Fig. 15 The six geometric errors of translational axis *Z* identified by the redundancy measurement method with sensitivity analysis. **a** Three translational errors. **b** Three rotational errors

Fig. 12, the results of positioning error deviation through general non-collinear three measurement lines method are compared to the result generated by the redundancy measurement method with sensitivity analysis. For the positioning errors of *Z*-axis, the maximum deviation is 1.32 and 0.38 μm, respectively. Compared with the result of positioning error deviation between generated and estimated for two measurement methods, the curve of estimated error identified by the redundancy measurement method with sensitivity analysis (discrepancies within 0.38 μm) are closer to the generated curve than the one identified by the general non-collinear three measurement lines method (discrepancies within 1.32 μm). The effectiveness of the proposed method for measuring the geometric error of linear axis is accordingly verified.

5.2 Experiment

To verify the effectiveness of the proposed method, a four-axis machine tool (shown in Fig. 13) was utilized to measure the geometric errors of translational axis *Z*. A laser interferometer (RENISHAW XL–80) was used to measure the geometric errors of axis *Z*. The translational range of translational axis *Z* is [− 60, 60] as shown in Table. 2. Before the measurement, the machine tool is warmed up for 20 min according to the standard warming-up procedure recommended in [26]. By applying the proposed method, the comprehensive geometric errors, including positioning errors and straightness errors of axis *Z* in a four-axis machine tool, are measured (shown in Fig. 14), and the installation diagram of the experiment is

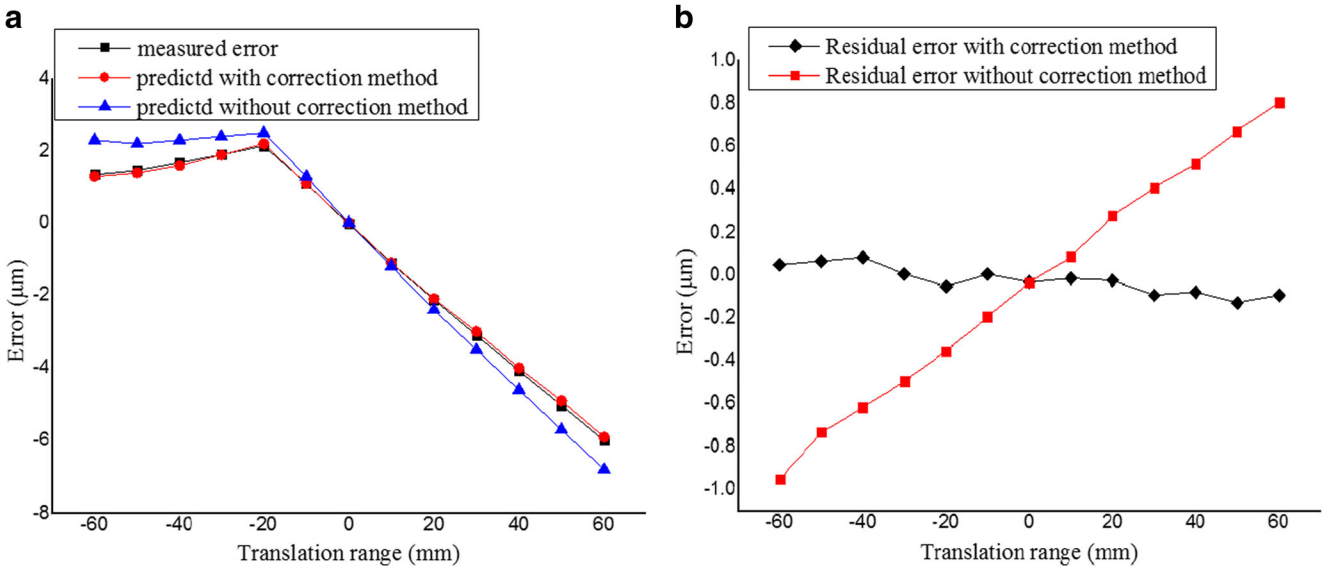

Fig. 16 Deviation between measured and predicted errors. **a** The predicted errors computing by redundancy method and redundancy method with sensitivity analysis. **b** The residual errors computing by redundancy method and redundancy method with sensitivity analysis

Table 1 The simulation parameters

Parameters		Unit	Given value
First measurement point		mm	$X = -120$, $Y = -60$, $Z = -30$
Translation range		mm	[− 60, 60]
Redundancy method parameter	H	mm	130
	W	mm	123
Redundancy method parameter with sensitivity analysis	H	mm	115
	W	mm	163
Set-up error (Δx_i, Δy_i, Δz_i)		mm	[− 3,3]

shown in Table. 2. The geometric errors calculation formulations are shown as Eq. 18. The identified geometric errors of axis Z using redundancy measurement method with sensitivity analysis are illustrated in Fig. 15. A correction NC code was implemented in a four-axis machine tool from the result of identified geometric errors of axis *Z*. Measured data, which show deviations from nominal position, are shown in Fig. 16.

As shown in the Fig. 16, the measured errors is the positioning error of translational axis *Z*. It can be seem that the values of positioning error of *Z*-axis are significantly improved by using two different methods, especially through the redundancy measurement method with sensitivity analysis. Through the sensitivity analysis, optimum installation position, which was not sensitive to the influence of the position error, has been chosen to measure geometrical error. Meanwhile, the positioning error of axis *Z* can be reduced from 5.94 to 0.18 μm with the proposed method within the measuring range of 120 mm after error compensation which shown in Fig. 16. A more precisely predicted result could be obtained by the method with sensitivity analysis especially for the high-precision occasion. Through the sensitivity analysis, optimum installation position can be figured out and the measurement result can be more accurate by conducting measurement in that optimum position which was not sensitive to the influence of the position errors. As shown in Fig. 16, it is obvious that when the data is far from the origin, the curve using the redundancy measurement method with sensitivity analysis fit better than the curve without sensitivity analysis. For the long distance, small estimate deviation of rotational error including (pitch, yaw, and roll) would cause a large magnitude of positioning error of axis *Z*. This is coincident with the conclusion drawn in Section 5.1.

6 Conclusion

In this paper, a mathematical redundancy identification method with sensitivity analysis is established through the multi-body system theory and the transformation matrix method. The installation position of the measurement instrument is presented in this study to investigate the factors which can affect the position errors of high-precision machine tools. Two experiments are conducted to study the effect of measurement strategies on the error identification to verify the developed position error sensitivity model. Based on the theoretical and experimental investigations, major findings are summarized as follows:

(i). The precision of the proposed error identification methodology is acceptable for precision machine tools;
(ii). Rotational error of translational axis should be paid more attention in a large stroke ultra-precision occasion;
(iii). Installation errors of the measurement system in some cases would have large influence on the identification result of geometric errors;
(iv). The comparison of the installation parameters (Table. 2) and the error identification precision (Fig. 14) between the first and the second experiment indicates that the adjust of the measurement lines helps to reduce the

Table 2 The installation parameters

Parameters		Unit	Given value
First measurement point		mm	$X = -70$, $Y = -50$, $Z = 30$
Translation range		mm	[− 60,60]
Redundancy method parameter	H	mm	40
	W	mm	110
Redundancy method parameter with sensitivity analysis	H	mm	90
	W	mm	100

influence of installation errors of the measurement system and improve the error identification precision;

(v). Positioning error of axis *Z* can be reduced dramatically with the method proposed in this article after error compensation.

Acknowledgements The authors would like to express their sincere thanks to the support of the National Natural Science Foundation of China (No. 51205067), Guangdong Innovative Research Team Program (No. 201001G0104781202) and Guangdong Science and Technology Planning Project (No. 2013B090500125, No. 2015B010101013, and No. 2015B010102012).

References

1. Chen JS, Yuan J, Ni J (1996) Thermal error modelling for real-time error compensation. Int J Adv Manuf Technol 12(4):266–275
2. Yang JG, Ren YQ, Liu GL, Zhao HT (2005) Testing, variable selecting and modeling of thermal errors on an INDEX-G200 turning center. Int J Adv Manuf Technol 26(7–8):814–818
3. Cui GW, Lu Y, Li JG (2012) Geometric error compensation software system for CNC machine tools based on NC program reconstructing. Int J Adv Manuf Technol 63(1–4):169–180
4. Kiridena VSB, Ferreira PM (1994) Parameter estimation and model verifacation of first order quasistatic error model for three-axis machining centers. Int J Mach Tools Manuf 34(1):101–125
5. Yi Z, Yang JG, Zhang K (2013) Geometric error measurement and compensation for the rotary table of five-axis machine tool with double ballbar. Int J Adv Manuf Technol 65(1–4):275–281
6. Schwenke H, Knapp W, Haitjema H (2008) Geometric error measurement and compensation of machines—an update. CIRP Ann Manuf Technol 57(2):660–675
7. Ibaraki S, Knapp W (2012) Indirect measurement of volumetric accuracy for three-axis and five-axis machine tools: a review. Int J Autom Technol 6(2):110–124
8. Lee JC, Lee HH (2016) Total measurement of geometric errors of a three-axis machine tool by developing a hybrid technique. Int J Precis Eng Man 17(4):427–432
9. ISO230-2 (2006) Test code for machine tools—Part 2: determination of accuracy and repeatability of positioning numerically controlled axes, ISO
10. Wei W, Kweon SH (2009) Development of an optical measuring system for integrated geometric errors of a three-axis miniaturized machine tool. Int J Adv Manuf Technol 43(7–8):701–709
11. Liu CH, Jywe WY (2005) Development of a laser-based high-precision six-degrees-of-freedom motion errors measuring system for linear stage. Rev Sci Instrum 76(5):055110–055110-6
12. Lee JH, Yang SH (2005) Measurement of geometric errors in a miniaturized machine tool using capacitance sensors. J Mater Process Technol 164-165(10):1402–1509
13. Gu T, Lin S (2016) An improved total least square calibration method for straightness error of coordinate measuring machine. Proc IMechE, Part B: J Engineering Manufacture 230(9):1665–1672
14. Okafor AC, Ertekin YM (2000) Derivation of machine tool error models and error compensation procedure for three axes vertical machining center using rigid body kinematics. Int J Mach Tools Manuf 40(8):1199–1213
15. Sergio A, David S, Jorge S (2012) Identification strategy of error parameter in volumetric error compensation of machine tool based on laser tracker measurements. Int J Mach Tools Manuf 53(1):160–169
16. Lee DM, Lee HH, Yang SH (2013) Analysis of squareness measurement using a laser interferometer system. Int J Precis Eng Man 14(10):1839–1840
17. Lee DM, Zhu ZK, Lee KL (2011) Identification and measurement of geometric errors for a five-axis machine tool with a tilting head using a double ball-bar. Int J Precis Eng Man 12(2):337–343
18. Lee KL, Lee JC, Yang SH (2014) Performance evaluation of five-DOF motion in ultra-precision linear stage. Int J Precis Eng Man 15(1):129–134
19. Chen GQ, Yuan JX, Ni J (2001) A displacement measurement approach for machine geometric error assessment. Int J Mach Tools Manuf 41(1):149–161
20. Wang JD, Guo JJ (2011) Method of geometric error identification for numerical control machine tool based on laser tracker. Chin J Mech Eng-En 47(14):13–19
21. Du Z, Zhang S (2010) Development of a multi-step measuring method for motion accuracy of NC machine tools based on cross grid encoder. Int J Mach Tools Manuf 50(3):270–280
22. Aguado S, Samper D (2012) Towards an effective identification strategy in volumetric error compensation of machine tools. Meas Sci Technol 23(6):207–207
23. Fan KC, Chen MJ (2000) A 6-degree-of-freedom measurement system for the accuracy of x-y stages. Precis Eng 24(1):15–23
24. Zhang Z, Hu H (2014) Measurement and compensation of geometric errors of three-axis machine tool by using laser tracker based on a sequential multilateration scheme. Proc IMechE, Part B: J Engineering Manufacture 228(8):819–831
25. Zhang Z, Hu H (2013) A general strategy for geometric error identification of multi-axis machine tools based on point measurement. Int J Adv Manuf Technol 69(5–8):1483–1497
26. ISO230-1 (2012) Test code for machine tools—Part 1: geometric accuracy of machines operating under no-load or quasi-static conditions. ISO
27. Donmez MA, Bloquist DS, Hocken RJ, Liu CR (1986) A general methodology for machine tool accuracy enhancement by error compensation. Precis Eng 8(4):187–196
28. Kong LB (2008) A kinematics and experimental analysis of form error compensation in ultra-precision machining. Int J Mach Tools Manuf 48(12–13):1408–1419
29. Lee RS, Lin YH (2012) Applying bidirectional kinematics to assembly error analysis for five- axis machine tools with general orthogonal configuration. Int J Adv Manuf Technol 62(9–12):1261–1272
30. Sabourin L, Robin V (2012) Improving the capability of a redundant robotic cell for cast parts finishing. Ind Robot 39(4):381–391
31. Corbel D, Company O (2010) Enhancing PKM accuracy by separating actuation and measurement. A 3DOF case study. J Mech Robot 2(3):191–220
32. Golub GH, Van Loan CF (2012) Matrix computations, fourth edn. Johns Hopkins University Press, Maryland